

Preparation, Characterization, and Antioxidant Activities of Cellulose Nanocrystals/Genistein Nanocomposites

Yue Wang,^a Yulong Wang,^{a,*} Yanxin Liu,^{a,b} Qingjian Liu,^a Jinwon Jang,^c and Junyuan Han^a

Genistein (GEN), a typical isoflavone compound, exhibits desirable pharmacological activities, such as antioxidation, anti-inflammatory, anti-angiogenesis, and anti-cancer properties. However, the pharmaceutical application of GEN is limited because of its poor water solubility in aqueous systems. In this study, cellulose nanocrystals (CNCs) and cetyltrimethylammonium bromide (CTAB)-coated CNCs were used as carriers for GEN to improve its dissolution rate and antioxidant activity in aqueous systems. The CNC/GEN and CNC/CTAB/GEN nanocomposites were successfully prepared and characterized by Fourier transform infrared spectroscopy, transmission electron microscopy, and X-ray diffraction analysis. The results showed that the nanonized GEN performed better and its crystalline structure decreased because of the formation of the CNC/GEN and CNC/CTAB/GEN nanocomposites. The GEN dissolution rates in the CNC/GEN and CNC/CTAB/GEN nanocomposites increased to 72.1% and 92.5% at 120 min, respectively, compared with that of the original GEN (0.85%). Furthermore, the *in vitro* antioxidant activity of the GEN, which was evaluated by the hydroxyl radical scavenging efficiency, was remarkably enhanced. Based on the above results, CNCs as nanocarriers are a useful method for improving the dissolution and antioxidant activities of GEN in aqueous system.

Keywords: Cellulose nanocrystals; Genistein; Nanocomposite; Dissolution rate; Antioxidation activity

Contact information: a: College of Chemical and Biological Engineering, Changsha University of Science and Technology, Changsha 410114, China; b: Key Laboratory of Pulp and Paper Science & Technology of Ministry of Education of China, Qilu University of Technology, Jinan 250353, China; c: Faculty of Medical Sciences, Dalhousie University, Halifax, Nova Scotia B3H 4R2, Canada;

* Corresponding author: wangyulong_1977@126.com

INTRODUCTION

Genistein (GEN) (4',5,7-trihydroxyisoflavone) is a natural polyphenolic compound. It is an important member of the isoflavone family and is extracted from many kinds of natural products, such as soybeans (Miura *et al.* 2002), the *Ginkgo biloba* leaf (Wang *et al.* 2007), and *Trifolium pratense* L. (Spagnuolo *et al.* 2014). Studies have demonstrated that GEN possesses many pharmacological activities, such as antioxidation (Han *et al.* 2009), anti-inflammatory (Danciu *et al.* 2012), anti-angiogenesis (Fotsis *et al.* 1995), and anti-cancer properties (Zhou *et al.* 2008). However, the pharmaceutical application of GEN is limited because of its poor water solubility and low lipid solubility. It has been reported that the water solubility of GEN is only 1.45 µg/mL and the pharmacological activities of GEN are seriously hampered while in an aqueous solution (Coldham *et al.* 2002; Wu *et al.* 2010).

To improve the bioavailability of GEN, many strategies have been proposed. For example, Daruházi *et al.* (2008) prepared a GEN-cyclodextrin inclusion complex and

enhanced the *in vitro* dissolution of GEN. Cohen *et al.* (2011) proposed high amylose corn starch as a carrier for GEN and improved both the *in vivo* and *in vitro* bioavailability and stability. Shimoda *et al.* (2011) revealed that the glycosylated products of GEN can improve the bioavailability of GEN and increase its radical scavenging activity.

Cellulose nanocrystals (CNCs), which are a few hundred nanometers in length and 10 nm to 20 nm in width, are a promising nano-scale biomaterial that is extracted from cellulose fibers, such as wood, straw, cotton, and ramie fibers (Azizi Samir *et al.* 2005; Azizi *et al.* 2013; Lin and Dufresne 2014). Cellulose nanocrystals show great potential as drug delivery carriers because of their excellent characteristics, including biodegradability, biocompatibility, non-toxicity, nano-scale size, and high chemical reactivity (Xu *et al.* 2018). Jackson *et al.* (2011) used CNCs as drug delivery excipients for hydrophobic anti-cancer drugs (paclitaxel, docetaxel, and etoposide) and found that controlled drug release could be achieved. Mohanta *et al.* (2014) investigated CNC-based microcapsules and thin films as the support for curcumin and enhanced its bioavailability and dispersity. In the previous study by the authors, 20(R)-ginsenoside Rg3 was successfully anchored onto CNCs based on the formation of hydrogen bonds and increased the hydroxyl radical (OH•) scavenging efficiency of 20(R)-ginsenoside Rg3 (Tang *et al.* 2017). To improve the hydrophobicity of CNCs, cetyltrimethylammonium bromide (CTAB) is commonly used for CNCs modification (Seabra *et al.* 2018); however, a low concentration of CTAB should be taken due to its potential damage to cell membranes (Ulitzur 1970).

In this study, CNCs were used as carriers for GEN to enhance its dissolution rate and antioxidant activity. The GEN was first nanonized through anti-solvent recrystallization and then loaded onto the CNCs to form the CNC/GEN nanocomposite. Moreover, the CNCs were coated with CTAB to increase their hydrophobicity during preparation of the CNC/CTAB/GEN nanocomposite. The resultant CNC/GEN and CNC/CTAB/GEN nanocomposites were characterized by Fourier transform infrared (FTIR) spectroscopy, transmission electron microscopy (TEM), and X-ray diffraction (XRD) analysis. The dissolution rate and *in vitro* antioxidant activity (OH• free radical scavenging) were also studied.

EXPERIMENTAL

Materials

The CNC was purchased from Cellulose Lab Inc. (Fredericton, Canada), where it was produced by a sulfuric acid hydrolysis method. The CNC obtained had a length of 100 nm to 250 nm, width of 5 nm to 20 nm, and zeta potential of -45 mV. The GEN (~98% purity) was purchased from Shanghai PureOne Biotechnology Co. Ltd. (Shanghai, China). Anhydrous ethanol, CTAB, salicylic acid, ferrous sulfate, and hydrogen peroxide were purchased from Shanghai Aladdin Biochemical Technology Co. Ltd. (Shanghai, China). All of the other chemicals were analytical reagents and used as received.

Methods

Preparation of the CNC/GEN nanocomposite

The CNC/GEN nanocomposite was prepared according to Tang *et al.* (2017). The original GEN was dissolved in anhydrous ethanol to form a solution with a concentration of 200 µg/mL under ultrasonic dispersion at room temperature. Subsequently, 3 mL of the GEN ethanol solution were added dropwise into a well-dispersed CNC aqueous solution

(30 mL and 0.1 wt.%) under vigorous stirring at 0 °C, which was maintained for 10 min. Finally, the resultant CNC/GEN nanocomposite suspension was freeze-dried for future use. For comparison, 3 mL of the GEN ethanol solution (200 µg/mL) were added dropwise into deionized water (30 mL) under the same conditions to prepare GEN particles without CNCs (traditional anti-solvent recrystallization process). Also, the original GEN was well-dispersed in 30 mL of deionized water at a concentration of 20 µg/mL to form the water-dispersed GEN sample.

Preparation of the CNC/CTAB/GEN nanocomposite

A CTAB solution with a concentration of 1 mmol/L was prepared by dissolving CTAB in deionized water. Five milliliters of the CTAB solution were added dropwise into 30 mL of CNC aqueous solution (0.1 wt.%) under magnetic stirring at room temperature. The resultant CNC/CTAB mixture was heated to 60 °C, which was maintained for 30 min under magnetic stirring, and then cooled down to room temperature. The reaction product obtained was centrifuged at 10000 rpm for 10 min to form a CTAB-modified CNC precipitate, which was then freeze-dried for subsequent use.

Three milliliters of the GEN ethanol solution (200 µg/mL) were added dropwise into a CTAB-modified CNC aqueous suspension (30 mL and 0.1 wt.%) under vigorous stirring at 0 °C, which was maintained for 10 min. The resultant CNC/CTAB/GEN nanocomposite suspension was freeze-dried for further use.

Characterization

The FTIR spectra of the samples were recorded on a Nicolet iS5 FTIR Spectrometer (Thermo Fisher, Waltham, MA, USA) in the transmittance mode. Thirty-six scans were collected over a range of 400 cm⁻¹ to 4000 cm⁻¹ with a resolution of 4 cm⁻¹. The samples were diluted with deionized water to a concentration of 0.01 mg/mL. A few drops of the diluted solution were placed on carbon-coated copper grids and air-dried overnight at room temperature. The TEM analysis was conducted using a JEM-2010 (S) microscope (JEOL, Tokyo, Japan) at an accelerating voltage of 200 kV. The XRD patterns were obtained on a Bruker D8 Advance X-ray Diffractometer (Karlsruhe, Germany) (40 kV and 25 mA). The diffraction intensity of the Cu K α radiation was measured over a 2 θ scanning range of 3° to 50° at 0.02°/s per step.

Dissolution rate measurement

The dissolution rate was measured in a phosphate buffer solution (PBS; pH = 7.4) at 37 °C using the paddle method (Kocbek *et al.* 2006). Two milligram samples of GEN were placed in 100 mL of PBS, and stirred at 100 rpm and 37 °C. At a prescheduled time, 5 mL of each sample were removed and filtered through a 0.22 µm membrane for ultraviolet (UV) absorption measurement at a wavelength of 260 nm to determine the GEN concentration. Then, 5 mL of fresh PBS were immediately added to the dissolution medium. The dissolution rate of GEN was calculated using Eq. 1,

$$\text{Dissolution rate (\%)} = (C_n \times V_2 + C_1 \times V_1 + C_2 \times V_1 + \dots + C_{n-1} \times V_1) \times 100\% / m \quad (1)$$

where C_1 , C_2 , C_{n-1} , and C_n are the GEN concentrations at a prescheduled time (mg/mL); m is the total input of GEN (mg); V_1 is the fixed sampling volume (mL); and V_2 is the total volume of dissolution medium (mL).

In vitro antioxidant activity

The *in vitro* antioxidant activity of the samples was evaluated by determining the OH• scavenging ability, according to the salicylic acid hydroxylation method (Smirnoff and Cumbes 1989). In this method, the Fenton reaction was used to generate OH•, which were then trapped by salicylic acid. The system consisted of 150 mM PBS (pH 7.4), 0.15 mM Fe³⁺-EDTA, 2 mM salicylic acid, 0.26 mM ascorbic acid, sample solution, and 0.6 mM H₂O₂. After incubating the mixture for 100 min at 37 °C, the UV absorption was measured at a wavelength of 530 nm. The OH• scavenging rate was calculated using Eq. 2,

$$\text{OH}\cdot \text{ scavenging rate (\%)} = (A_c - A_s) \times 100\% / A_c \quad (2)$$

where A_c is the UV absorbance of the control, representing the total amount of OH• generated, and A_s is the UV absorbance of the sample.

RESULTS AND DISCUSSION

Concept of Preparing the CNC/GEN and CNC/CTAB/GEN Nanocomposites

The flow chart for preparing the CNC/GEN and CNC/CTAB/GEN nanocomposites is shown in Fig. 1.

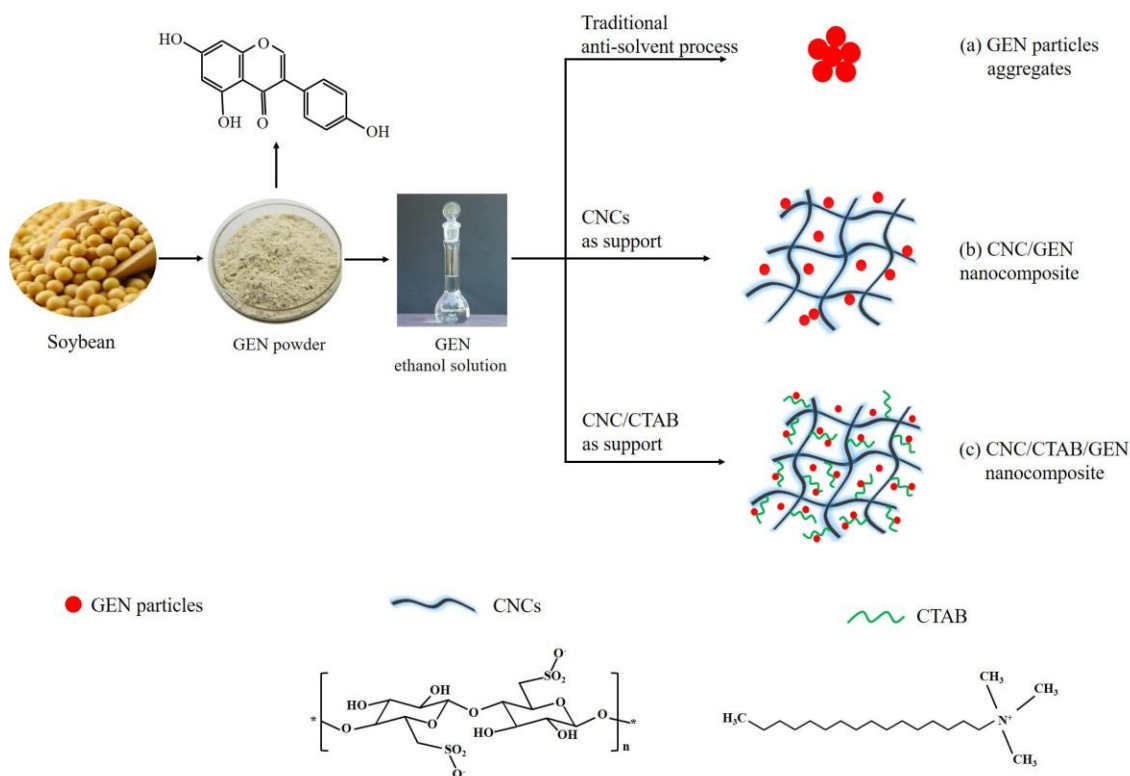


Fig. 1. Schematic illustration of the formation of the CNC/GEN and CNC/CTAB/GEN nanocomposites

In the traditional anti-solvent recrystallization process (Fig. 1), a GEN ethanol solution was added dropwise into deionized water, and the volume of solvent (ethanol) to

anti-solvent (deionized water) was 1:10. The GEN formed nuclei at a supersaturated concentration in the anti-solvent, and then the precipitated material continued to grow into nanoparticles. Because of its hydrophobic nature, the GEN nanoparticles flocculated and formed aggregates, which are difficult to disperse in aqueous solutions. As carriers, CNCs provided more sites for the GEN nuclei because of their large surface area and abundant hydrogen bonds, which resulted in the formation of smaller and even GEN nanoparticles (Fig. 1). Moreover, the excellent hydrophilicity of the CNCs allowed the CNC/GEN system to be quite stable, which lowered the flocculation and aggregation of the resultant GEN nanoparticles. Dalvi and Dave (2009) reported that the use of polymers and surfactants as stabilizers can inhibit/low the particle growth of hydrophobic griseofulvin, such as poly(vinylpyrrolidone), hydroxypropyl methyl cellulose, Tween 80, and sodium dodecyl sulfate. After CTAB modification, the CNCs became more hydrophobic and had a better compatibility with the GEN molecules because of the presence of long carbon chains of CTAB. It was easier to load GEN nanoparticles on the CNCs *via* electrostatic and hydrophobic interactions (Fig. 1), which can further lower the particle size and improve the stability of the GEN nanoparticles.

FTIR Analysis

The FTIR spectra of the original GEN, CNC, CNC/GEN composite, and CNC/CTAB/GEN composite are shown in Fig. 2. The original GEN showed typical absorption peaks at 1650 cm^{-1} (C=O stretching), 1611 cm^{-1} and 1517 cm^{-1} (C=C skeletal vibrations), 1306 cm^{-1} (C-OH bending vibration), 1200 cm^{-1} (C=O=C stretching vibration), and 840 cm^{-1} and 810 cm^{-1} (C-H bending vibration). Similar FTIR absorption peaks for GEN were also observed by Crupi *et al.* (2007). For the CNCs, the characteristic peaks were observed at 3340 cm^{-1} (O-H stretching), 2910 cm^{-1} (C-H stretching), 1055 cm^{-1} (secondary hydroxyl), 1030 cm^{-1} (primary hydroxyl), and 890 cm^{-1} (vibration of cellulose anomeric carbon), which agreed with those reported previously (Yu *et al.* 2012).

In contrast, for the CNC/GEN nanocomposite, the hydroxyl band (attributed to the CNCs) at 3330 cm^{-1} increased and shifted slightly to a lower wavenumber region compared with that of the CNCs, which was attributed to the formation of hydrogen bonds between the CNCs and GEN. Moreover, typical absorption peaks of the GEN were found in the CNC/GEN nanocomposite, which indicated that the GEN was successfully loaded onto the CNCs.

For the CNC/CTAB/GEN nanocomposite, the absorption peak at 2910 cm^{-1} (overlapping of $-\text{CH}_2$ from the CNCs and CTAB) was attributed to the attachment of long alkyl chains from the CTAB onto the CNCs. The new absorption peak observed at 1463 cm^{-1} was because of quaternary ammonium groups, which indicated that the CNCs were successfully coated with CTAB. Zainuddin *et al.* (2017) obtained similar results after the modification of kenaf nanocrystalline cellulose with CTAB. Again, the hydroxyl absorption at 3330 cm^{-1} in the CNC/CTAB/GEN nanocomposite was shifted slightly to a lower wavenumber region compared with that of the CNCs; furthermore, the peak intensity of the hydroxyl was stronger than that of the CNC/GEN nanocomposite, which indicated the formation of hydrogen bonds between the CNCs and GEN. Moreover, typical absorption peaks of the GEN appeared in the CNC/CTAB/GEN nanocomposite, which confirmed that the GEN was successfully loaded onto the CNCs.

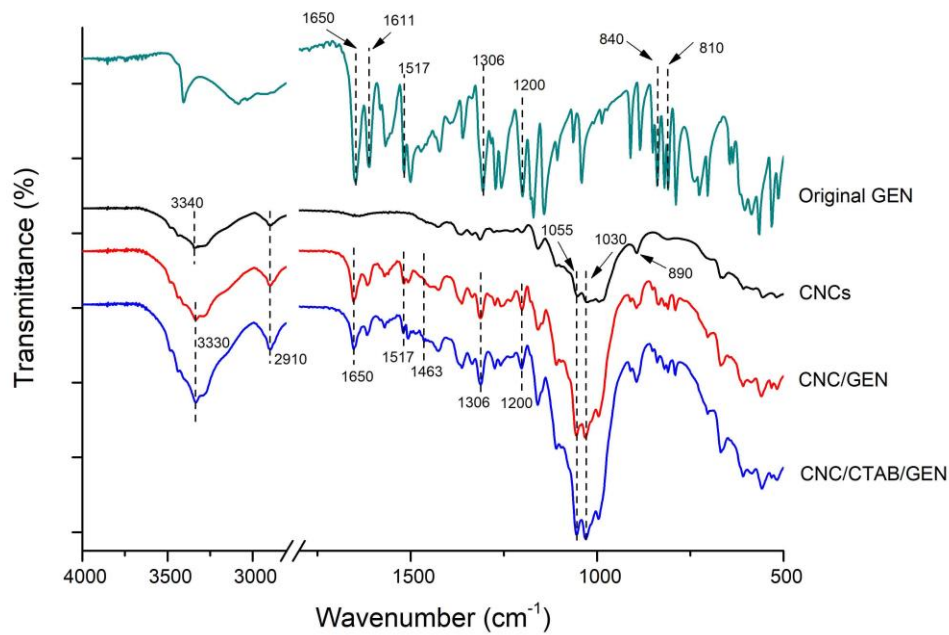


Fig. 2. FTIR spectra of the original GEN, CNCs, CNC/GEN nanocomposite, and CNC/CTAB/GEN nanocomposite

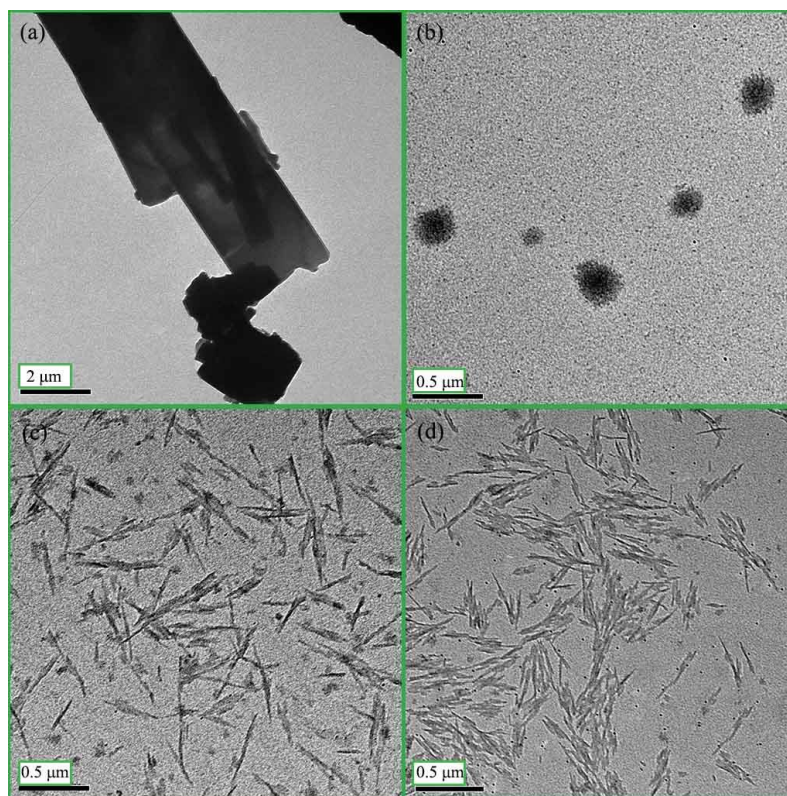


Fig. 3. TEM images of the (a) water-dispersed GEN; (b) GEN particles (traditional anti-solvent recrystallization process); (c) CNC/GEN nanocomposite; and (d) CNC/CTAB/GEN nanocomposite (slight flocculation of the CTAB-coated CNCs because of the enhanced hydrophobicity)

TEM Morphology

Figure 3 shows the TEM images of the water-dispersed GEN, GEN particles, CNC/GEN nanocomposite, and CNC/CTAB/GEN nanocomposite.

The water-dispersed GEN was in a crystalline state and had a large particle size (Fig. 3a). The GEN particles prepared by the traditional anti-solvent precipitation process aggregated with a particle size range of 80 nm to 220 nm (Fig. 3b), which were difficult to further disperse in the aqueous solution because of the hydrophobic nature of the GEN.

In contrast, the aggregates of the GEN particles were well dispersed into a number of small and even sized nanoparticles during the formation of the CNC/GEN nanocomposite (Fig. 3c). Moreover, the GEN was further dispersed and nanonized by means of forming the CNC/CTAB/GEN nanocomposite (Fig. 3d), which was attributed to the increased hydrophobicity of the CNCs (slight flocculation of the CNCs) after the CTAB modification. The nanonization of a hydrophobic drug can help to enhance its dissolution rate and bioavailability because of the increased specific surface area (Chen *et al.* 2011).

These results confirmed that as carriers, the CNCs and CTAB-modified CNCs were effective at dispersing the GEN in the aqueous solution, while maintaining the system stability with the formation of nanocomposites, which agreed with the present hypothesis.

XRD Analysis

The XRD patterns of the original GEN, GEN particles, CNCs, CNC/GEN nanocomposite, and CNC/CTAB/GEN nanocomposite are shown in Fig. 4. The original GEN displayed intense diffraction peaks at 2θ values of 7.5° , 12.1° , 12.6° , 14.3° , 15.0° , 16.5° , 18.0° , 22.5° , and 24.7° (Fig. 4), which indicated that it was in a crystalline state. The GEN particles made by the traditional anti-solvent precipitation process (without CNCs), showed intense diffraction peaks at 2θ values of 7.5° , 12.1° , 12.6° , 14.3° , and 24.7° , but these peak intensities were lower compared with that of the original GEN.

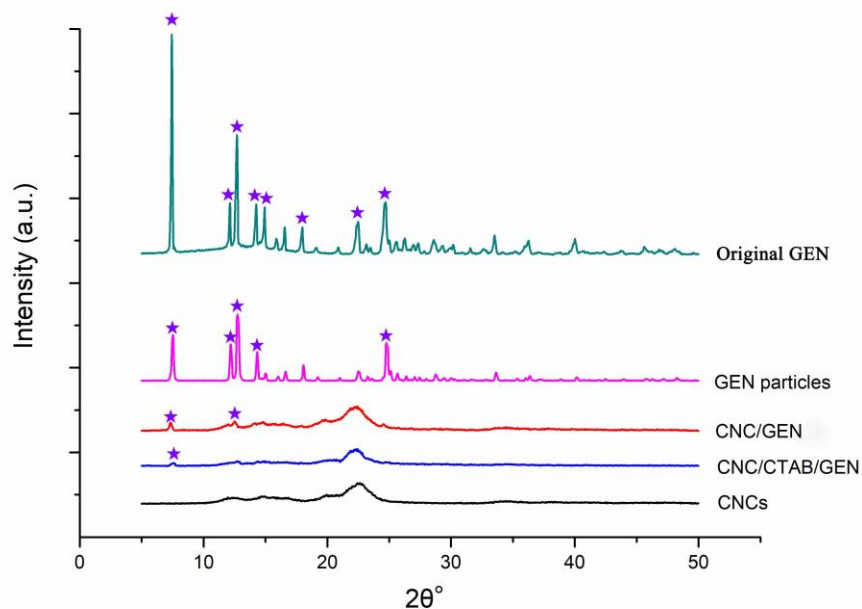


Fig. 4. XRD patterns of the original GEN, GEN particles (traditional anti-solvent recrystallization process), CNC/GEN nanocomposite, CNC/CTAB/GEN nanocomposite, and CNCs

In contrast, for the CNC/GEN nanocomposite, most of the diffraction peaks of the GEN disappeared and only two weak diffraction peaks at 2θ values of 7.5° and 12.6° were observed, which were attributed to the GEN. Moreover, for the CNC/CTAB/GEN nanocomposite, only one weak diffraction peak at a 2θ of 7.5° was observed, which was attributed to the GEN, and the other GEN diffraction peaks disappeared. These results demonstrated that the GEN changed from a highly crystalline state to a low crystalline state (nearly amorphous state) based on the formation of the CNC/GEN and CNC/CTAB/GEN nanocomposites. The improved nanonization of the GEN could have been responsible for the decrease in the crystalline state. Cai *et al.* (2017) transformed the crystalline structure of GEN into an amorphous structure by loading the GEN into chitosan particles, which enhanced the water solubility of the GEN.

Dissolution Rate

The dissolution rates of the original GEN, GEN particles, CNC/GEN nanocomposite, and CNC/CTAB/GEN nanocomposite were studied, and the results are shown in Fig. 5. The original GEN had a limited dissolution rate, only 0.85% at 120 min. During the dispersing process, most of the original GEN particles, which were difficult to make wet, floated on the surface of the PBS because of the hydrophobic nature of the GEN. Compared with the original GEN, the dissolution rate of the GEN particles increased and was 14.2% at 120 min. This was because the GEN was nanonized during the traditional anti-solvent recrystallization process, which increased the specific surface area and dissolution rate of the GEN.

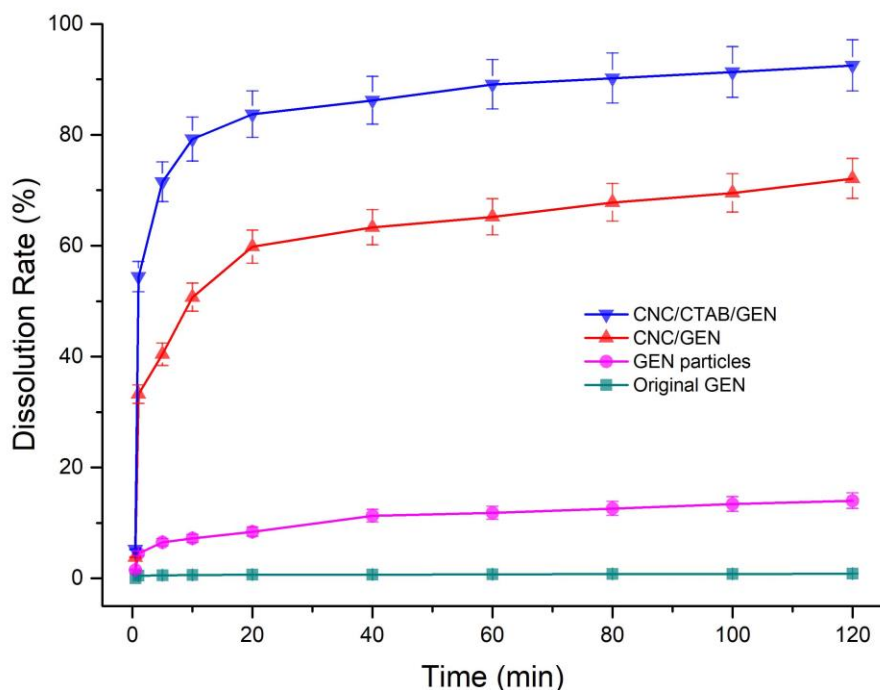


Fig. 5. Dissolution rates of the CNC/CTAB/GEN nanocomposite, CNC/GEN nanocomposite, GEN particles (traditional anti-solvent recrystallization process), and original GEN

In contrast, for the CNC/GEN and CNC/CTAB/GEN nanocomposites, the dissolution rates of the GEN clearly increased. For example, the dissolution rates of the GEN in the CNC/GEN and CNC/CTAB/GEN nanocomposites reached 50.7% and 79.2% in the first 10 min, respectively; subsequently, the dissolution rates increased slowly and reached 72.1% and 92.5% at 120 min, respectively. The dissolution rate is well related to the bioavailability of hydrophobic drugs. In the literature, many researchers have reported that the bioavailability of hydrophobic drugs, such as quercetin (Wu *et al.* 2008) and curcumin (Yen *et al.* 2010), can be effectively enhanced by increasing their dissolution rate.

***In vitro* Antioxidant Activity**

The OH•, which is the most toxic free radical, is a typical reactive oxygen species that is well related to many kinds of diseases, such as heart disease, diabetes, and liver injury (Jaeschke 2000; Giordano 2005; Rolo and Palmeira 2006). In this study, the OH• scavenging rate was used to evaluate the *in vitro* antioxidant activity of the GEN and the results are shown in Fig. 6.

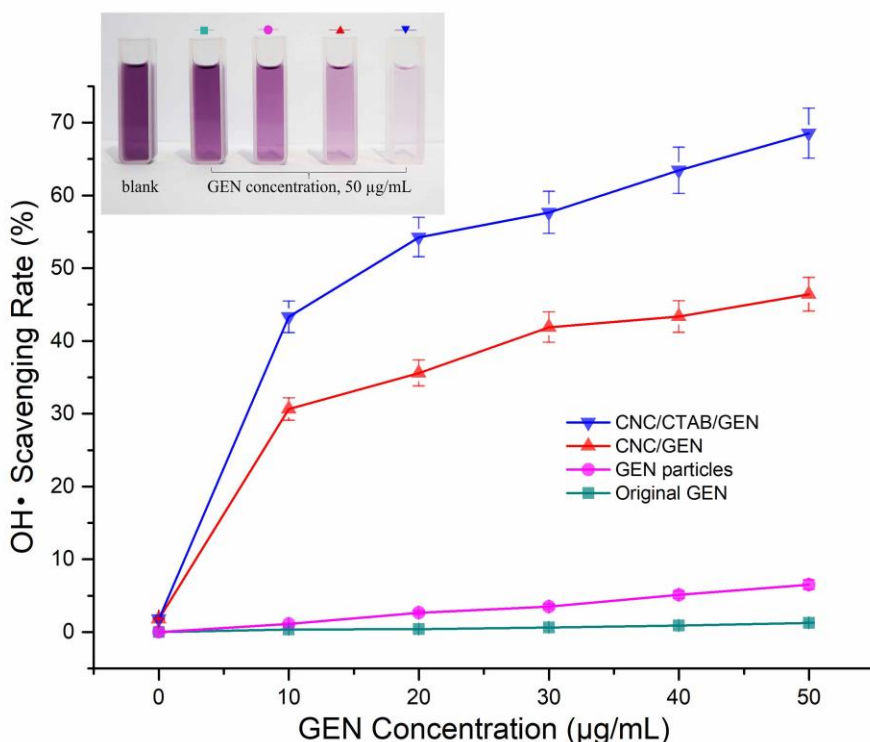


Fig. 6. OH• scavenging rates of the CNC/CTAB/GEN nanocomposite, CNC/GEN nanocomposite, GEN particles (traditional anti-solvent recrystallization process), and original GEN (The image embedded shows the color contrast of OH• scavenging systems when different samples were used, and the lighter color was related to the higher OH• scavenging rate)

The OH• scavenging rate of the original GEN was quite low, only 1.3% at a 50 µg/mL concentration. For the GEN particles, the OH• scavenging rate increased and reached 6.5% at a 50 µg/mL concentration. In contrast, for the CNC/GEN and CNC/CTAB/GEN nanocomposites, the OH• scavenging rates obviously increased and were 30.6% and 43.3% at a 10 µg/mL concentration, respectively, and then increased to

46.4% and 68.5% at a 50 µg/mL concentration, respectively. The CNC/CTAB/GEN nanocomposite had the highest OH• scavenging rate at the same GEN concentration, which was attributed to the enhanced hydrophobicity and compatibility with the GEN after the CTAB modification of the CNCs. It was found that the OH• scavenging rates of the samples showed similar a trend to that of the dissolution rates, which indicated that a higher dissolution rate contributes to an increase in the OH• scavenging rate.

CONCLUSIONS

1. The nanocomposites cellulose nanocrystal/genistein (CNC/GEN) and the same with cetyltrimethylammonium chloride (CNC/CTAB/GEN) were successfully prepared by the formation of hydrogen bonds (between the CNCs and GEN) and electrostatic interactions (between the CTAB chain and GEN).
2. The results from the transmission electron microscopy (TEM) and X-ray diffraction (XRD) analyses showed that the dispersity, compatibility, and nanonization of the GEN in the aqueous solution were remarkably enhanced, and that the GEN changed from a highly crystalline state to a low crystalline state (nearly amorphous state) because of the formation of the CNC/GEN and CNC/CTAB/GEN nanocomposites.
3. The dissolution rates of the GEN in the CNC/GEN and CNC/CTAB/GEN nanocomposites increased to 72.1% and 92.5% at 120 min, respectively, compared with that of the original GEN (0.85%). Furthermore, the *in vitro* antioxidant activity of the GEN, which was evaluated by the OH• scavenging efficiency, was obviously enhanced.
4. The prepared CNC/GEN and CNC/CTAB/GEN nanocomposites can be useful for the improvement of the dissolution and antioxidant activities of GEN because of the facile preparation method and good biocompatibility.

ACKNOWLEDGMENTS

The authors gratefully acknowledge the financial support of the Open Fund of Key Laboratory of Pulp and Paper Science & Technology of the Ministry of Education of China and Qilu University of Technology (Grant No. 08031340). The authors would also like to thank Mr. Steven R. Cogswell and Dr. Ven Reddy from University of New Brunswick (Fredericton, Canada) for their help with the TEM and XRD analyses.

REFERENCES CITED

- Azizi, S., Ahmad, M., Mahdavi, M., and Abdolmohammadi, S. (2013). "Preparation, characterization, and antimicrobial activities of ZnO nanoparticles/cellulose nanocrystal nanocomposites," *BioResources* 8(2), 1841-1851. DOI: 10.15376/biores.8.2.1841-1851
- Azizi Samir, M. A. S., Alloin, F., and Dufresne, A. (2005). "Review of recent research into cellulosic whiskers, their properties and their application in nanocomposite field," *Biomacromolecules* 6(2), 612-626. DOI: 10.1021/bm0493685

- Cai, L., Yu, R., Hao, X., and Ding, X. (2017). "Folate receptor-targeted bioflavonoid genistein-loaded chitosan nanoparticles for enhanced anticancer effect in cervical cancers," *Nanoscale Res. Lett.* 12(1), 509. DOI: 10.1186/s11671-017-2253-z
- Chen, H., Khemtong, C., Yang, X., Chang, X., and Gao, J. (2011). "Nanonization strategies for poorly water-soluble drugs," *Drug Discov. Today* 16(7-8), 354-360. DOI: 10.1016/j.drudis.2010.02.009
- Cohen, R., Schwartz, B., Peri, I., and Shimoni, E. (2011). "Improving bioavailability and stability of genistein by complexation with high-amylose corn starch," *J. Agr. Food Chem.* 59(14), 7932-7938. DOI: 10.1021/jf2013277
- Coldham, N. G., Zhang, A.-Q., Key, P., and Sauer, M. J. (2002). "Absolute bioavailability of [¹⁴C] genistein in the rat; plasma pharmacokinetics of parent compound, genistein glucuronide and total radioactivity," *Eur. J. Drug Metab. Ph.* 27(4), 249-258. DOI: 10.1007/BF03192335
- Crupi, V., Ficarra, R., Guardo, M., Majolino, D., Stancanelli, R., and Venuti, V. (2007). "UV-vis and FTIR-ATR spectroscopic techniques to study the inclusion complexes of genistein with β -cyclodextrins," *J. Pharmaceut. Biomed.* 44(1), 110-117. DOI: 10.1016/j.jpba.2007.01.054
- Dalvi, S. V., and Dave, R. N. (2009). "Controlling particle size of a poorly water-soluble drug using ultrasound and stabilizers in antisolvent precipitation," *Ind. Eng. Chem. Res.* 48(16), 7581-7593. DOI: 10.1021/ie900248f
- Danciu, C., Soica, C., Csanyi, E., Ambrus, R., Feflea, S., Peev, C., and Dehelean, C. (2012). "Changes in the anti-inflammatory activity of soy isoflavonoid genistein versus genistein incorporated in two types of cyclodextrin derivatives," *Chem. Cent. J.* 6(1), 58. DOI: 10.1186/1752-153X-6-58
- Daruházi, Á. E., Szente, L., Balogh, B., Mátyus, P., Béni, S., Takács, M., Gergely, A., Horváth, P., Szőke, É., and Lemberkovic, É. (2008). "Utility of cyclodextrins in the formulation of genistein: Part 1. Preparation and physicochemical properties of genistein complexes with native cyclodextrins," *J. Pharmaceut. Biomed.* 48(3), 636-640. DOI: 10.1016/j.jpba.2008.06.007
- Fotsis, T., Pepper, M., Adlercreutz, H., Hase, T., Montesano, R., and Schweigerer, L. (1995). "Genistein, a dietary ingested isoflavonoid, inhibits cell proliferation and *in vitro* angiogenesis," *J. Nutr.* 125(S3), 790S-797S. DOI: 10.1093/jn/125.suppl_3.790S
- Giordano, F. J. (2005). "Oxygen, oxidative stress, hypoxia, and heart failure," *J. Clin. Invest.* 115(3), 500-508. DOI: 10.1172/JCI24408
- Han, R.-M., Tian, Y.-X., Liu, Y., Chen, C.-H., Ai, X.-C., Zhang, J.-P., and Skibsted, L. H. (2009). "Comparison of flavonoids and isoflavonoids as antioxidants," *J. Agr. Food Chem.* 57(9), 3780-3785. DOI: 10.1021/jf803850p
- Jackson, J. K., Letchford, K., Wasserman, B. Z., Ye, L., Hamad, W. Y., and Burt, H. M. (2011). "The use of nanocrystalline cellulose for the binding and controlled release of drugs," *Int. J. Nanomed.* 6, 321-330. DOI: 10.2147/IJN.S16749
- Jaeschke, H. (2000). "Reactive oxygen and mechanisms of inflammatory liver injury," *J. Gastroen. Hepatol.* 15(7), 718-724. DOI: 10.1046/j.1440-1746.2000.02207.x
- Kocbek, P., Baumgartner, S., and Kristl, J. (2006). "Preparation and evaluation of nanosuspensions for enhancing the dissolution of poorly soluble drugs," *Int. J. Pharm.* 312(1-2), 179-186. DOI: 10.1016/j.ijpharm.2006.01.008
- Lin, N., and Dufresne, A. (2014). "Nanocellulose in biomedicine: Current status and future prospect," *Eur. Polym. J.* 59, 302-325. DOI: 10.1016/j.eurpolymj.2014.07.025

- Miura, T., Yuan, L., Sun, B., Fujii, H., Yoshida, M., Wakame, K., and Kosuna, K. I. (2002). "Isoflavone aglycon produced by culture of soybean extracts with basidiomycetes and its anti-angiogenic activity," *Biosci. Biotech. Bioch.* 66(12), 2626-2631. DOI: 10.1271/bbb.66.2626
- Mohanta, V., Madras, G., and Patil, S. (2014). "Layer-by-layer assembled thin films and microcapsules of nanocrystalline cellulose for hydrophobic drug delivery," *ACS Appl. Mater. Inter.* 6(22), 20093-20101. DOI: 10.1021/am505681e
- Rolo, A. P., and Palmeira, C. M. (2006). "Diabetes and mitochondrial function: Role of hyperglycemia and oxidative stress," *Toxicol. Appl. Pharm.* 212(2), 167-178. DOI: 10.1016/j.taap.2006.01.003
- Seabra, A. B., Bernardes, J. S., Fávoro, W. J., Paula, A. J., and Durán, N. (2018). "Cellulose nanocrystals as carriers in medicine and their toxicities: A review," *Carbohydr. Polym.* 181, 514-527. DOI: 10.1016/j.carbpol.2017.12.014
- Shimoda, K., Kubota, N., Hamada, H., and Hamada, H. (2011). "Synthesis of gentiooligosaccharides of genistein and glycitein and their radical scavenging and anti-allergic activity," *Molecules* 16(6), 4740-4747. DOI: 10.3390/molecules16064740
- Smirnoff, N., and Cumbes, Q. J. (1989). "Hydroxyl radical scavenging activity of compatible solutes," *Phytochemistry* 28(4), 1057-1060. DOI: 10.1016/0031-9422(89)80182-7
- Spagnuolo, P., Rasini, E., Luini, A., Legnaro, M., Luzzani, M., Casareto, E., Carreri, M., Paracchini, S., Marino, F., and Cosentino, M. (2014). "Isoflavone content and estrogenic activity of different batches of red clover (*Trifolium pratense* L.) extracts: An *in vitro* study in MCF-7 cells," *Fitoterapia* 94, 62-69. DOI: 10.1016/j.fitote.2014.01.027
- Tang, C., Wang, Y., Long, Y., An, X., Shen, J., and Ni, Y. (2017). "Anchoring 20(R)-ginsenoside Rg3 onto cellulose nanocrystals to increase the hydroxyl radical scavenging activity," *ACS Sustain. Chem. Eng.* 5(9), 7507-7513. DOI: 10.1021/acssuschemeng.6b02996
- Ulitzur, S. (1970). "The transport of β -galactosides across the membrane of permeaseless *Escherichia coli* ML35 cells after treatment with cetyltrimethylammonium bromide," *Biochim. Biophys. Acta, Biomembr.* 211(3), 533-541. DOI: 10.1016/0005-2736(70)90258-0
- Wang, F., Jiang, K., and Li, Z. (2007). "Purification and identification of genistein in *Ginkgo biloba* leaf extract," *Chin. J. Chromatogr.* 25(4), 509-513. DOI: 10.1016/S1872-2059(07)60019-4
- Wu, J.-G., Ge, J., Zhang, Y.-P., Yu, Y., and Zhang, X.-Y. (2010). "Solubility of genistein in water, methanol, ethanol, propan-2-ol, 1-butanol, and ethyl acetate from (280 to 333) K," *J. Chem. Eng. Data* 55(11), 5286-5288. DOI: 10.1021/je100261w
- Wu, T.-H., Yen, F.-L., Lin, L.-T., Tsai, T.-R., Lin, C.-C., and Cham, T.-M. (2008). "Preparation, physicochemical characterization, and antioxidant effects of quercetin nanoparticles," *Int. J. Pharm.* 346(1-2), 160-168. DOI: 10.1016/j.ijpharm.2007.06.036
- Xu, Y., Li, S., Yue, X., and Lu, W. (2018). "Review of silver nanoparticles (AgNPs)-cellulose antibacterial composites," *BioResources* 13(1), 2150-2170. DOI: 10.15376/biores.13.1.2150-2170
- Yen, F.-L., Wu, T.-H., Tzeng, C.-W., Lin, L.-T., and Lin, C.-C. (2010). "Curcumin nanoparticles improve the physicochemical properties of curcumin and effectively

- enhance its antioxidant and antihepatoma activities,” *J. Agr. Food Chem.* 58(12), 7376-7382. DOI: 10.1021/jf100135h
- Yu, M., Yang, R., Huang, L., Cao, X., Yang, F., and Liu, D. (2012). “Preparation and characterization of bamboo nanocrystalline cellulose,” *BioResources* 7(2), 1802-1812. DOI: 10.15376/biores.7.2.1802-1812
- Zainuddin, N., Ahmad, I., Kargarzadeh, H., and Ramli, S. (2017). “Hydrophobic kenaf nanocrystalline cellulose for the binding of curcumin,” *Carbohydr. Polym.* 163, 261-269. DOI: 10.1016/j.carbpol.2017.01.036
- Zhou, H.-B., Chen, J.-M., Cai, J.-T., Du, Q., and Wu, C.-N. (2008). “Anticancer activity of genistein on implanted tumor of human SG7901 cells in nude mice,” *World J. Gastroentero.* 14(4), 627-631. DOI: 10.3748/wjg.14.627

Article submitted: August 3, 2018; Peer review completed: October 20, 2018; Revised version received and accepted: November 16, 2018; Published: November 20, 2018.
DOI: 10.15376/biores.14.1. 336-348